JACS
JOURNAL OF THE AMERICAN CHEMICAL SOCIETY
pubs.acs.org/JACS
Article

Cu-Catalyzed Three-Component Alkene Carboamination: Mechanistic Insights and Rational Design to Overcome Limitations

Tam D. Ho,[§] Byung Joo Lee,[§] Travis L. Buchanan, Micah E. Heikes, Ryan M. Steinert, E. Grace Milem, Sean T. Goralski, Ya-Nong Wang, SangHyun Lee, Vincent M. Lynch, Michael J. Rose, Katie R. Mitchell-Koch,* and Kami L. Hull*

Cite This: J. Am. Chem. Soc. 2024, 146, 25176−25189

Read Online

ACCESS | Metrics & More | Article Recommendations | Supporting Information

ABSTRACT: Herein, we report mechanistic investigations into the Cu-catalyzed three-component carboamination of alkenes with α-halo carbonyls and aryl amines via an oxocarbenium intermediate. Monitoring the reaction reveals the formation of transient atom transfer radical addition (ATRA) intermediates with both electron-neutral and deficient vinyl arenes as well as unactivated alkenes. Based on our experimental studies and density functional theory calculations, the oxocarbenium is generated through atom transfer and subsequent intramolecular substitution. Further, mechanistic factors that dictate the regioselectivity of the nucleophilic attack onto the oxocarbenium to afford the γ-amino ester, γ-iminolactone, or γ-lactone are discussed. A strategy to overcome scope limitation with respect to unactivated alkenes is developed using the mechanistic insights gained herein. Finally, we demonstrate that under modified conditions, our Cu catalyst enables the ATRA reaction between a variety of alkyl halides and vinyl arenes/α-olefins, and we present a one-pot, two-step carbofunctionalization with an array of nucleophiles through ATRA/S_N2.

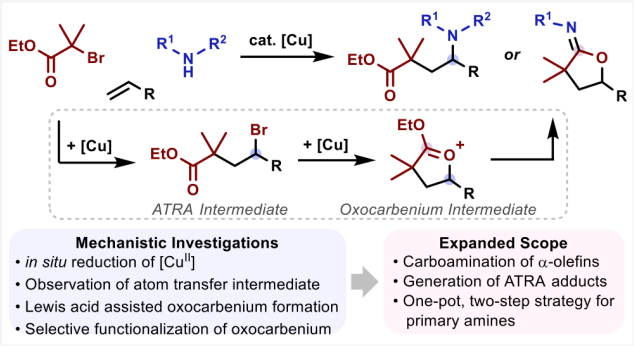

INTRODUCTION

The development of innovative methodologies for the efficient synthesis of organic small molecules lies at the heart of modern organic chemistry. Given the ubiquity of C−N bonds in biologically active molecules, devising improved methods for their synthesis is a pivotal objective. Olefin difunctionalization offers direct access to complex molecular frameworks in a single step. Within this approach, the carboamination of alkenes represents a significant subset, as it simultaneously incorporates both carbon and nitrogen functionalities into the substrate (Scheme 1a).[1−3] For these reasons, our group, along with several others, has conducted extensive research to develop versatile approaches for olefin carboamination.[4−26] These strategies require preactivated carbon[17] or nitrogen[19] components and are limited in their olefin scope to either electron-rich/electron-neutral vinyl arenes[17,18,26] or electron-deficient/strained alkenes[19] (Scheme 1b).

Recently, we presented a more general copper-catalyzed carboamination strategy joining α-halo carbonyls and secondary aryl amines with styrene derivatives (Scheme 2a).[4,27] Notably, electron-rich, electron-deficient, and internal vinyl arenes participate (**1**−**5**). Further, secondary and tertiary α-halo carbonyls undergo the carboamination reaction to afford the corresponding γ-aminocarbonyls. However, we observe several limitations: only electron-deficient primary anilines afford carboamination products in the reactions with styrene (**7** and **8**), iminolactones predominate in reactions involving electron-rich and -neutral anilines (**9**), and unactivated alkenes also result in the formation of iminolactones selectively (**10** and **11**). Finally, readily reducible radical precursors lacking the carbonyl group, e.g., Cl_3CBr, do not participate in the reaction.[28]

In our recently developed Cu-catalyzed carboamination reaction, the necessity of the carbonyl functional group along with the competing carboamination and iminolactonization reactions led us to the mechanistic hypothesis shown in Scheme 2b. The proposed catalytic cycle begins with (i) reduction of the α-halo carbonyl **12** by [Cu^I] to generate [Cu^{II}]−Br and a carbon-centered radical **13**[29] that subsequently undergoes (ii) radical addition to the alkene to form radical adduct **14**.[30] Then, (iii) the [Cu^{II}] oxidizes **14** to the oxocarbenium **15** regenerating the [Cu^I] active catalyst.[31−33] Finally, (iv) nucleophilic attack by the amine at C1

Received: July 2, 2024
Revised: August 12, 2024
Accepted: August 13, 2024
Published: August 28, 2024

https://doi.org/10.1021/jacs.4c08945
J. Am. Chem. Soc. 2024, 146, 25176−25189

Scheme 1. Three-Component Carboamination Approaches

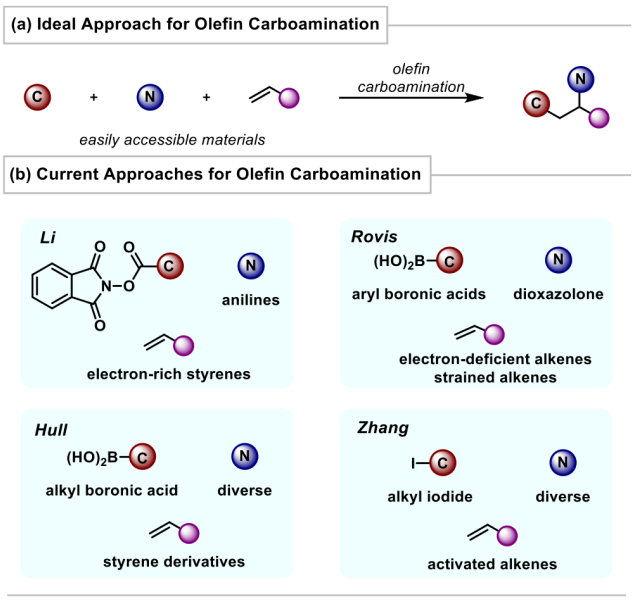

or C4 affords the carboamination product **16** or iminolactone **17**, respectively.

The carbonyl of the alkyl halide is requisite for the formation of the oxocarbenium intermediate **15** and facilitates the reaction with electronically diverse olefins. This neighboring group-stabilized carbocation intermediate is further supported by the observed lactonization in the reaction of the *t*-butyl *α*-bromoisobutyrate (**18**) with styrene (**19**) and *N*-methyl-*p*-toluidine (**20**). The lactone product **22** is formed along with the *N*-alkylation byproduct, detected by GCMS (Scheme 3a).[4] Upon the formation of the oxocarbenium intermediate, the S_N1/E1 reaction occurs preferentially at the *t*-butyl group (C5) to generate a stable *t*-butyl cation over the nucleophilic attack at either C1 or C4.

With this proposed catalytic cycle in mind, we hypothesized that replacing the ethyl ester with an Evans auxiliary **23** would promote a diastereoselective carboamination reaction. However, we observed olefin-dependent diastereoselectivity (Scheme 3b); *p*-MeO-styrene affords the carboamination product in 1.3:1 dr, styrene in 3:1 dr, and *p*-CF_3-styrene in 8:1 dr. In fact, there is a linear correlation between log [dr(X)/dr(H)] and σ with a ρ value of 0.8. As the steric interactions within the oxocarbeniums are not substantially influenced by the *para*-substituent on the aromatic ring, the observed impact of electronics on the diastereoselectivity suggests that the mechanism may be more complex than we initially hypothesized.

We sought to gain better insight into the mechanism of this carboamination reaction to overcome current limitations and guide the development of additional carbofunctionalization reactions. Herein, we present (1) how the active [Cu^I] catalyst is generated, (2) the mechanism for the formation of the oxocarbenium, and (3) the factors that control the regioselectivity of the nucleophilic attack onto the oxocarbenium intermediate. Finally, we apply these insights to significantly expand the scope of our carbofunctionalizations.

Scheme 2. Cu-catalyzed Carboamination and Mechanistic Insights

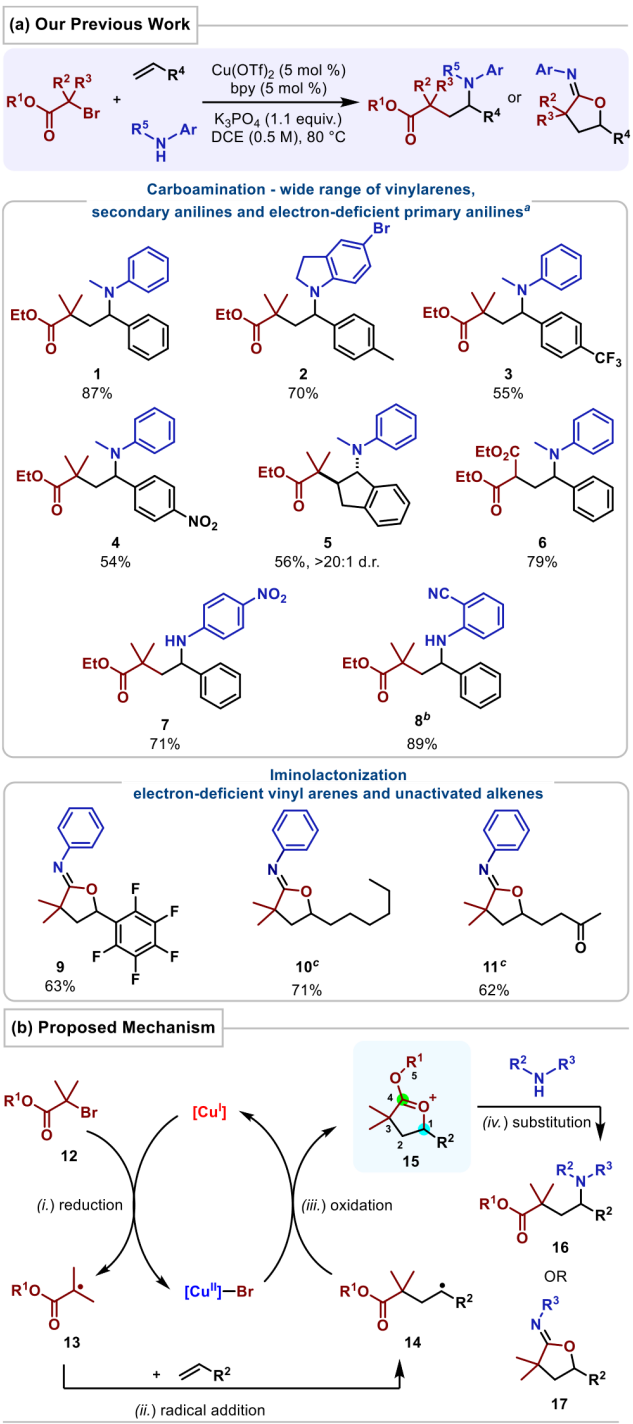

[a]$Cu(OTf)_2$ (5 mol %), bpy (5 mol %), K_3PO_4 (1.1 equiv), alkyl halide (2.0 equiv), vinyl arene (1.0 equiv), amine (1.0 equiv), and DCE (0.5 M), 80 °C, 24 h. [b][$Cu(dtbbpy)_2$]$(OTf)_2$ (1.5 mol %) instead. [c]Alkyl halide (2.0 equiv), alkene (3.0 equiv), and amine (1.0 equiv) instead.

RESULTS AND DISCUSSION

Active Catalyst Formation. First, we investigated how the proposed [Cu^I] active catalyst is formed. Our initially optimized reaction conditions rely on *in situ* generation of the catalyst: $Cu(OTf)_2$ (5.0 mol %) and 2,2′-bipyridine (bpy,

https://doi.org/10.1021/jacs.4c08945
J. Am. Chem. Soc. 2024, 146, 25176−25189

Scheme 3. Observation of Lactonization and Diastereoselectivity Using Chiral Auxiliary Halide[a]

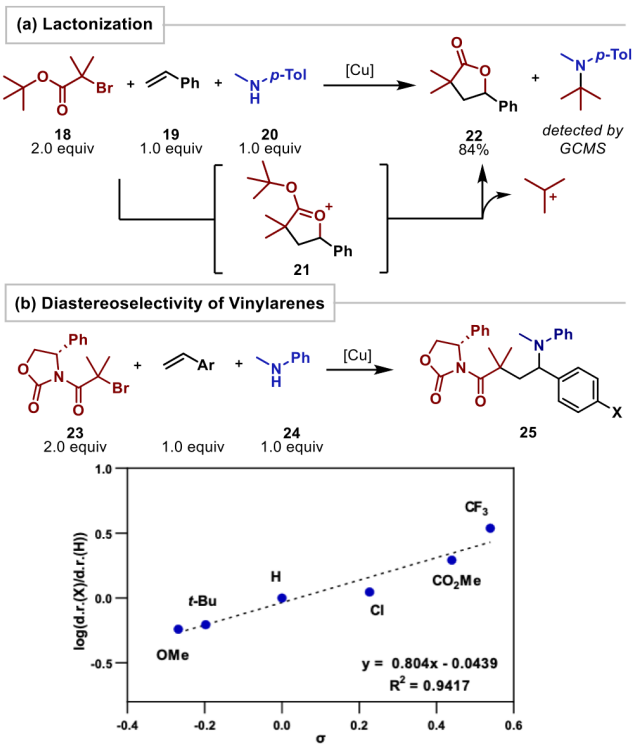

[a]See Supporting Information for reaction conditions.

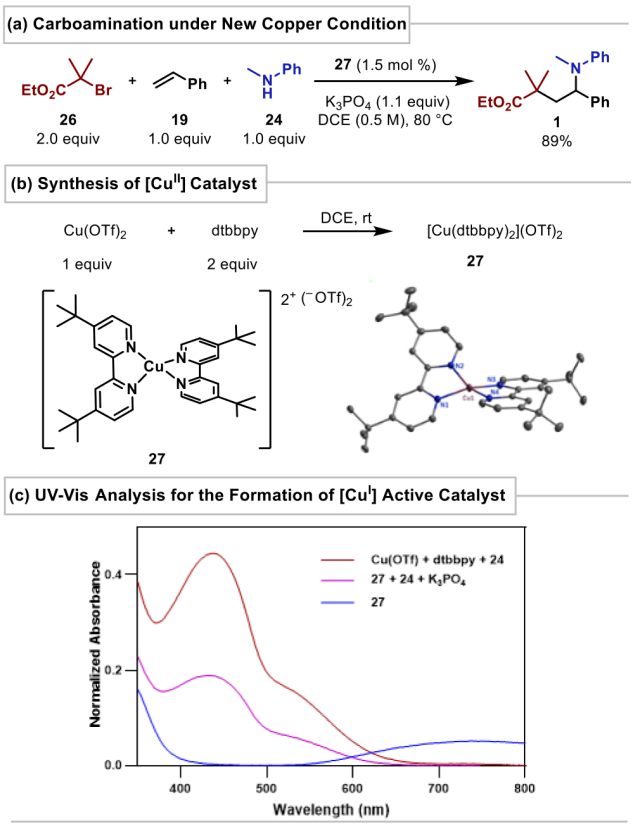

Figure 1. Carboamination utilizing the [Cu^{II}] complex and the observation of [Cu^{I}] active catalyst formation.

5.0 mol %) are added to the reaction along with all other reagents.[4] However, $Cu(OTf)_2$ and bpy ligand are slow to dissolve in 1,2-dichloroethane (DCE), leading to inconsistent reaction rates and varying induction periods when monitoring the carboamination reaction over time. We hypothesized that a precomplexed copper catalyst with solubilizing *t*-butyl groups might improve its solubility and, therefore, the kinetic profile. Indeed, $[Cu(dtbbpy)_2](OTf)_2$ (dtbbpy = 4,4′-di-*tert*-butyl-2,2′-bipyridine) (**27**) is a superior catalyst: it is soluble in DCE, only requires 1.5 mol % to afford complete conversion to carboamination product **1** (Figure 1a), and has a negligible induction period. The X-ray crystal structure of **27** reveals a distorted square planar [Cu^{II}] complex (Figure 1b).[34]

Observing the Reduction of [Cu^{II}] to [Cu^{I}] by EPR. The reduction of ethyl α-bromoisobutyrate (**26**) requires a [Cu^{I}] active catalyst, leading us to hypothesize that [Cu^{II}] complex **27** is reduced to [$Cu^{I}(dtbbpy)_2$]OTf under the reaction conditions by either inner- or outer-sphere reduction by *N*-methylaniline **24** and/or K_3PO_4.[35,36] Initially, we monitored this reaction by electron paramagnetic resonance spectroscopy (EPR). It is important to note that this analytical method can only observe paramagnetic species and is therefore selective for [Cu^{II}] (S = 1/2) species and organic radicals (S = 1/2); any [Cu^{I}] species formed are diamagnetic and, therefore, EPR silent. As such, we aimed to monitor the disappearance of the [Cu^{II}] EPR signal to gain insight into reduction. The [Cu^{II}] complex **27**, when frozen in DCE, exhibits an EPR spectrum typical for an axially symmetric [Cu^{II}] complex (g_x = 2.065 and $g_y = g_z$ = 2.255) (Figure S48).

Next, we sequentially added the other components of the reaction and determined their effect on **27**. In the presence of **24**, the g-tensor values for the features in the spectrum associated with the [Cu^{II}] complex show a significant shift toward rhombic (g_x = 1.996, g_y = 2.137, and g_z = 0.212), perhaps indicating ligation of *N*-methylaniline to $[Cu^{II}(dtbbpy)_2]^{2+}$ to afford $[Cu^{II}(dtbbpy)_2(NHMePh)]^{2+}$. Additionally, a second isotropic feature was observed (g_{iso} = 2.00084). As no strong hyperfine coupling was seen in these two isotropic signals, it was unlikely that this unpaired electron was delocalized across either the dtbbpy ligand or the aniline aromatic systems. Rather, it was localized on the nitrogen of *N*-methylaniline. This supports that the formation of the active [Cu^{I}] catalyst in this reaction proceeds by inner-sphere reduction of $[Cu^{II}(dtbbpy)_2]^{2+}$ by *N*-methylaniline, through $[Cu^{II}(dtbbpy)_2(NHMePh)]^{2+}$, to afford $[Cu^{I}(dtbbpy)_2]^{+}$ and an *N*-centered radical ($[\bullet NHMePh]^{+}$ or •NMePh). Subsequent dimerization occurs as hydrazine is detected by high-resolution mass spectrometry (HRMS) both in the stoichiometric reduction of **27** and in our standard reaction conditions (Figures 1a and S42).

Observing Reduction of [Cu^{II}] to [Cu^{I}] by UV−vis. Given the complexity of the EPR analysis, we sought an additional approach to monitor the reduction of [Cu^{II}] precatalyst **27**. The UV−vis spectrum of $[Cu(dtbbpy)_2](OTf)_2$ shows a band at 750 nm (Figure 1c). Upon addition of K_3PO_4 and *N*-methylaniline, a rapid color change is observed. The resulting solution by UV−vis has lost the band at 750 nm, and a new metal-to-ligand charge-transfer band appears at 432 nm. This observation supports the reduction of [Cu^{II}] to [Cu^{I}]. Likewise, $Cu^{I}OTf$ and dtbbpy (1:2) in the presence of *N*-methylaniline have a similar spectrum with an λ_{max} of 438 nm. It is worth noting that the UV−vis spectrum of the solution of CuOTf and dtbbpy is significantly different, suggesting that the

https://doi.org/10.1021/jacs.4c08945
J. Am. Chem. Soc. 2024, 146, 25176−25189

Scheme 4. Potential Carboamination Mechanisms

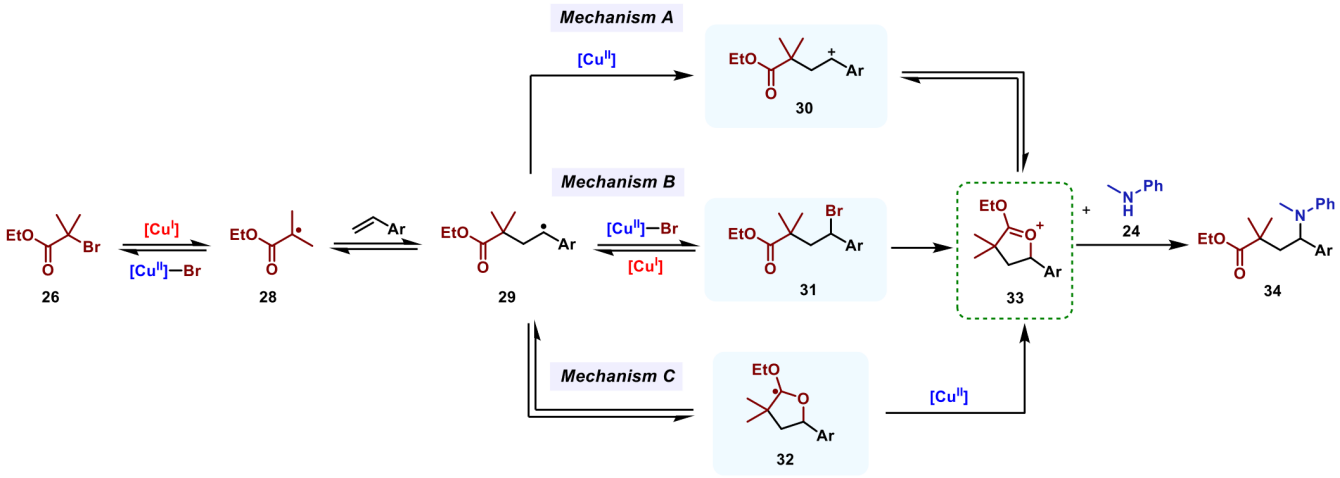

[Cu^{I}] complex in the reaction potentially coordinates to an *N*-methylaniline ligand (Figure S43). Notably, both *p*-trifluoromethylaniline and aniline promote analogous reduction of **27** and afford [Cu^{I}] with similar λ_{max}, 439 and 437 nm, respectively (Figure S43). Due to the instability of the [Cu^{I}] complex, we were unable to obtain X-ray quality crystals for determining the exact structure of the [Cu^{I}] complex.

Mechanistic Investigations into the Catalytic Cycle. We hypothesize that there are three generalized mechanisms, as shown in Scheme 4, for the Cu-catalyzed carboamination of a vinyl arene with ethyl α-bromoisobutyrate (**26**) and *N*-methylaniline (**24**) via oxocarbenium intermediate **33**.[4] This versatile intermediate could be generated through: **Mechanism A**—oxidation of benzylic radical **29**, followed by the cyclization of the ester onto benzylic carbocation **30**,[31−33] **Mechanism B**—bromine atom transfer from [Cu^{II}]−Br to **29** and subsequent intramolecular S_N2[37] between the ester and benzylic bromide of **31**,[32,38] or **Mechanism C**—5-*endo*-trig radical cyclization of **29** and oxidation of the resulting acetal radical (**32**).[39]

Determination of the Rate Equation. Initially, our focus was to identify the rate-determining step of the carboamination reaction. We obtained the following experimental rate law equation via comparison of the initial rates of reactions after systematically varying the reagent concentrations.

$$\text{rate} = k_{obs}\,[\mathbf{26}]\,[\mathbf{19}]\,[\mathbf{27}]\,[\mathbf{24}]^{0.4}$$

The reaction is first order in ethyl α-bromoisobutyrate (**26**), styrene (**19**), and [Cu^{II}] complex **27**. The observed fractional order, with respect to *N*-methylaniline **24**, suggests that multiple mechanisms may be operative under our reaction conditions.

Observation of the ATRA Intermediate. Careful analysis of our reaction profile reveals the formation and consumption of a stable intermediate in the model reaction. The intermediate was identified as the atom transfer radical addition (ATRA) adduct by mass spectrometry and further confirmed by independent synthesis and full characterization. As seen in Figure 2a, at early reaction times (<10 min), atom transfer adduct **35** is the major product; however, by 15 min, carboamination product **1** dominates (Figure 2a). Density functional theory (DFT) analysis supports that the ATRA adduct is thermodynamically favorable as **35** is 19.5 kcal mol^{-1} more stable than ethyl α-bromo isobutyrate **26** and styrene **19**. Notably, by the end of the reaction, no **35** remains. Importantly, observation of the ATRA intermediate is consistent with **Mechanism B**; however, given that benzylic

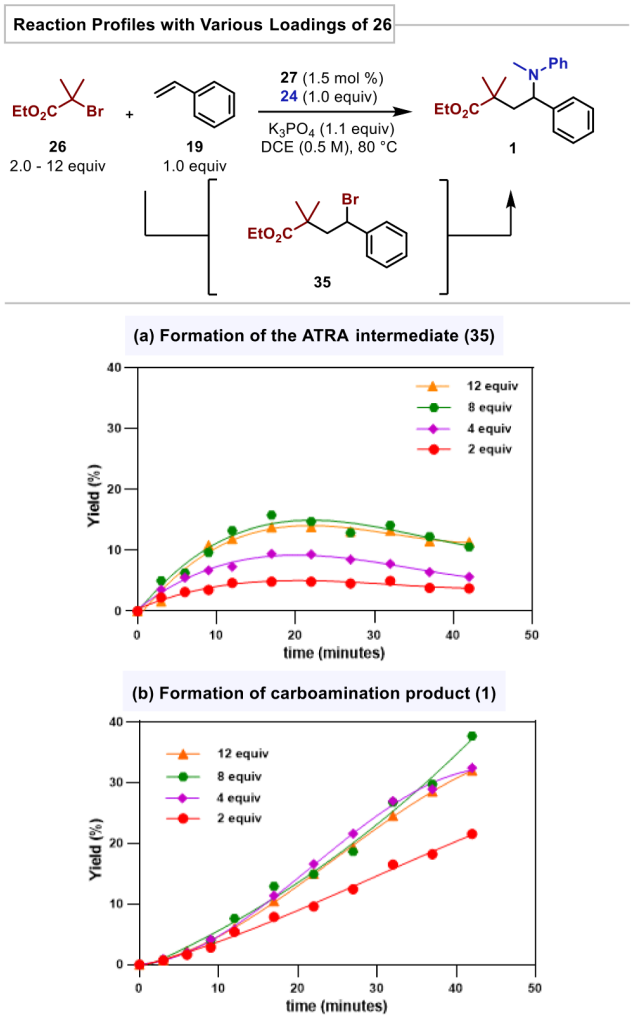

Figure 2. Observation of stable ATRA intermediates in the Cu-catalyzed carboamination reaction.

https://doi.org/10.1021/jacs.4c08945
J. Am. Chem. Soc. 2024, 146, 25176−25189

bromide is readily reduced to regenerate **29**, its formation does not eliminate either **Mechanisms A** or **C**.

We investigated the impact of the concentration of **26** on the relative rates of atom transfer vs carboamination. Increasing the concentration of **26** increases both the rate of the ATRA reaction and its maximum *in situ* yield (Figure 2a). Interestingly, the rate of carboamination increases from 2.0 to 4.0 equiv of **26** and does not further increase at 8.0 or 12 equiv (Figure 2b), suggesting that the reaction has reached saturation.

Substrate Influences on ATRA Formation. The relative rates of ATRA vs carboamination depend on the *para*-substituent on styrene. For example, the maximum *in situ* yield for the ATRA adduct **35** is 5% at 15 min; with *p*-CF_3-styrene (**36**), the maximum yield of **37** (33%) is observed after 60 min (Figure 3). A similar trend is observed with electronically

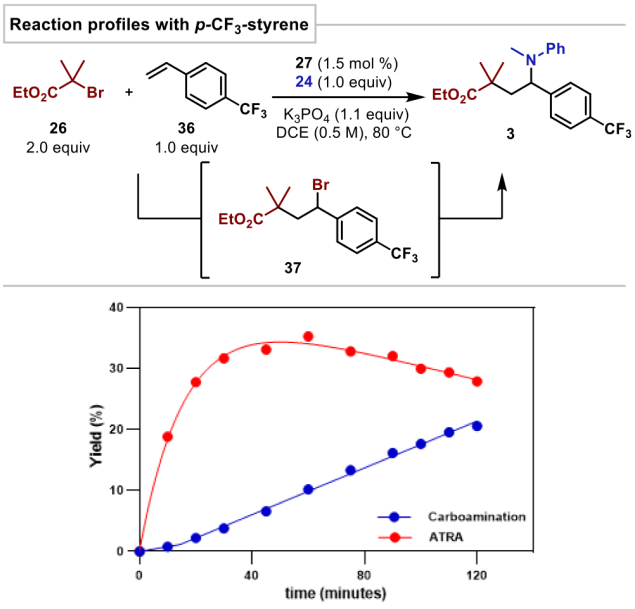

Figure 3. Observation of ATRA intermediates in the Cu-catalyzed carboamination reaction with *p*-CF_3-styrene.

diverse aryl esters; electron-deficient aryl esters rapidly form the ATRA adducts and are slow to undergo the amination step, while electron-rich analogs are slower in the ATRA reaction and faster in the subsequent carboamination (Table S2). On the other hand, with electron-rich styrene derivatives, no ATRA adducts are detected; rather, other side processes, consistent with carbocation intermediates, occur. For example, with *p*-MeO-styrene (**38**), in addition to 87% of **39**, we observe the formation of the carboarylation product **40** in 7% yield (Scheme 5). This isomer is likely formed through electrophilic aromatic substitution (EAS) with the *N*-methylaniline and suggests that *p*-MeO-styrene may be going through S_N1 or asynchronous S_N2 (vide infra). Notably, trace EAS products are observed with *p*-Me- and *p*-^{t}Bu-styrene, in 1.5 and 0.4% in situ yield, respectively, and are not observed with more electron-deficient styrene derivatives. Given the relative lack of EAS, it is likely that moderately electron-rich to electron-deficient vinyl arenes do not go through free-carbocation intermediates, and **Mechanism A** is not occurring.

Hammett Studies. We conducted a Hammett investigation as we hypothesized that cation/oxocarbenium formation is the

Scheme 5. Observation of the Carboarylation Product in Reaction with *p*-MeO-Styrene

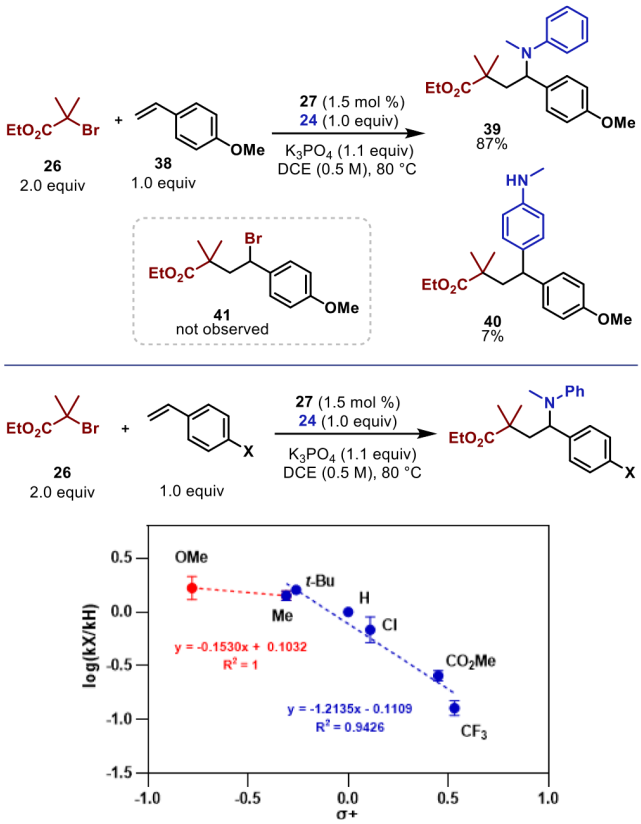

Figure 4. Hammett studies of Cu-catalyzed three-component carboamination.

rate-determining step. The nonlinear Hammett plot obtained, as shown in Figure 4, is consistent with a change in the rate-determining step. Electron-rich vinyl arenes have a ρ value of −0.2. This minimal ρ suggests that ATRA may be rate-determining followed by rapid substitution and aligns with not being able to detect the ATRA intermediate under our reaction conditions with *p*-MeO-styrene. The carboamination reaction with electron-neutral to electron-deficient vinyl arenes has a ρ value of −1.2. This supports that there is positive charge build-up in the rate-determining step. The moderate magnitude of the observed ρ value indicates that **Mechanism A** is not occurring, as we would anticipate a large negative ρ value (−5 to −6) for the formation of a free carbocation and suggests that oxocarbenium (**33**) formation is likely rate-determining.[40] However, the disparity in rates by which the ATRA intermediate is generated and consumed significantly complicates the conclusive analysis of this Hammett investigation. As such, we endeavored to study the mechanism of amination of the ATRA intermediate directly.

Amination of the ATRA Intermediate. As ATRA adduct **31** is generally a stable intermediate in our carboamination reaction, studying the mechanism of its amination will give us key mechanistic insights. First, we determined if copper catalyzes the amination of ATRA adduct **36**. In the absence of the copper catalyst, amination does occur, supporting **Mechanism B**. However, in the presence of [Cu^{II}] complex **27**, the reaction is 7.8 times faster than the background reaction (Scheme 6). This indicates that the uncatalyzed

https://doi.org/10.1021/jacs.4c08945
J. Am. Chem. Soc. 2024, 146, 25176−25189

Scheme 6. Relative Rate of ATRA Intermediate Amination

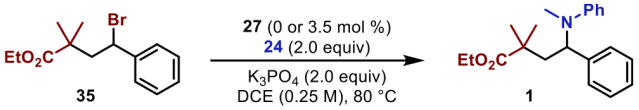

amination of ATRA adducts (**Mechanism B**) occurs and that the Cu-catalyzed amination is dominant.

Mechanism of the Uncatalyzed Amination. There are two possible pathways for amination of **31** via **33**: S_N1 (**mech 1**) or S_N2 (**mech 2**) (Scheme 7). We performed a Hammett study to determine the impact of electronically differentiated arenes on the rates of the reactions. As shown in Figure 5, a negative ρ value is observed ($\rho = -3.1$), consistent with the reaction proceeding through an S_N2 cyclization mechanism to afford a charged intermediate rather than S_N1, where a $\rho < -5$ is anticipated.[40]

Scheme 7. Possible Mechanisms for Uncatalyzed Amination

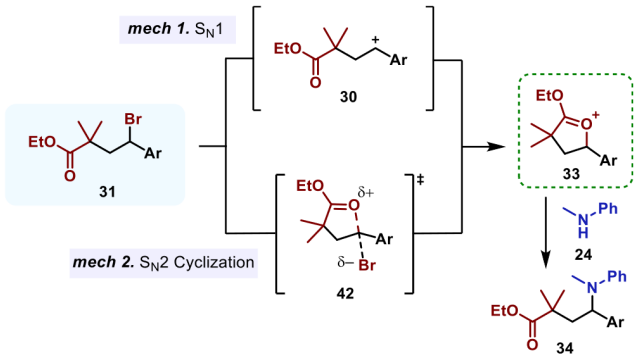

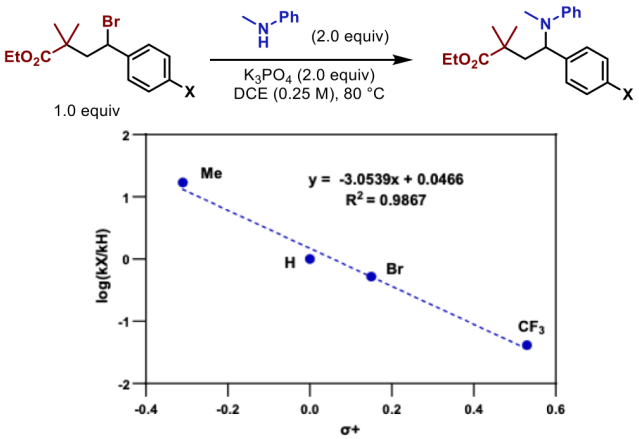

Figure 5. Hammett study of uncatalyzed animation.

We sought to further support that **mech 2** is the dominant pathway by determining the Thorpe-Ingold effect, the stereospecificity, and through DFT transition state analysis. If S_N1 is occurring (**mech 1**), formation of **30**, the benzylic carbocation, is likely the rate-determining step; thus, oxocarbenium formation is after the rate-determining step, and substitution adjacent to the carbonyl, increasing the Thorpe-Ingold effect, will not affect the rate of the reaction. However, if an S_N2 cyclization (**mech 2**) is occurring, the Thorpe-Ingold effect should increase the rate of α,α-dimethyl substrate **35** relative to α-methyl substrate **43**.[41,42] Indeed, **35** undergoes the amination about 2.6 times faster than **43**, supporting that the oxocarbenium forms via a neighboring group-assisted S_N2 (**mech 2**) (Scheme 8a). Additionally, we

Scheme 8. Mechanistic Studies on Background Amination

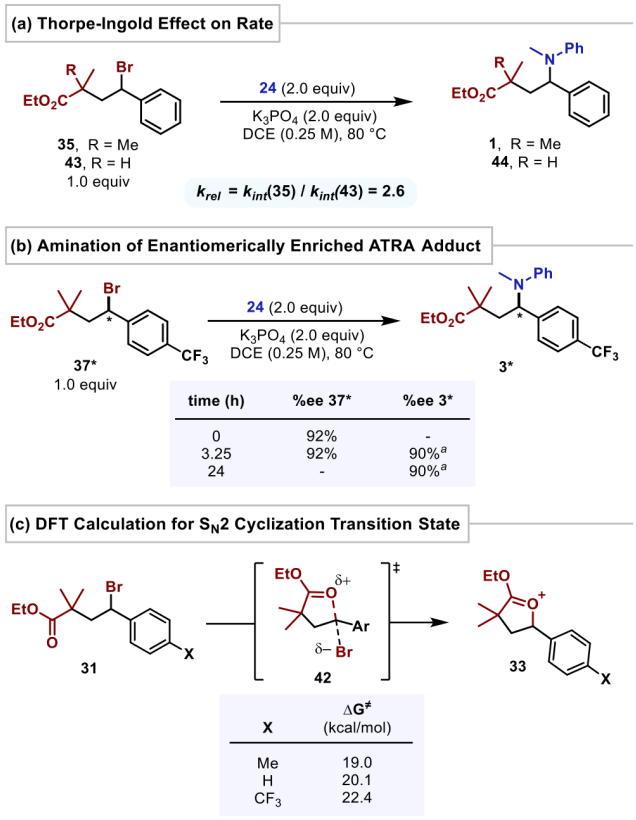

[a]Approximate % ee; see Supporting Information for more details.

subjected a single enantiomer, **37***, to the amination conditions and observed that the reaction is stereospecific as **3*** forms as a single enantiomer (Scheme 8b). Finally, DFT analysis of this intramolecular S_N2 to afford **33** (X = H) measures a $\Delta G^{\ddagger}$ of 20.1 kcal/mol, a reasonable energy barrier for our reaction conditions (80 °C) (Scheme 8c). Combined, these experiments support that the background amination is occurring through **mech 2** (Scheme 7).

Mechanism of Cu-Catalyzed Amination. Next, we investigated the mechanism of the Cu-catalyzed amination of the ATRA adducts. We propose that there are four possible mechanisms for this process, as outlined in Scheme 9. We hypothesize two possible roles for the copper catalyst in the formation of the oxocarbenium intermediate. One possibility is that the [Cu] complex is acting as a Lewis acid, binding to the Br and catalyzing the oxocarbenium formation via either S_N1 (**mech 1′**) or S_N2 (**mech 2′**).[43] Alternatively, as in **mech 3′**, the [Cu^I] reduces **31** to form benzylic radical **29** which undergoes a 5-*endo*-trig cyclization, generating the cyclic acetal radical **32**. Subsequent oxidation by [Cu^{II}] affords oxocarbenium **33**.[39] Finally, in **mech 4′**, a concerted reduction/cyclization occurs to generate cyclic acetal radical **32** and [Cu^{II}] directly; oxidation by [Cu^{II}] generates the oxocarbenium and regenerates the [Cu^I] catalyst.

https://doi.org/10.1021/jacs.4c08945
J. Am. Chem. Soc. 2024, 146, 25176−25189

Scheme 9. Possible Mechanisms for the Cu-catalyzed Amination of ATRA Intermediates

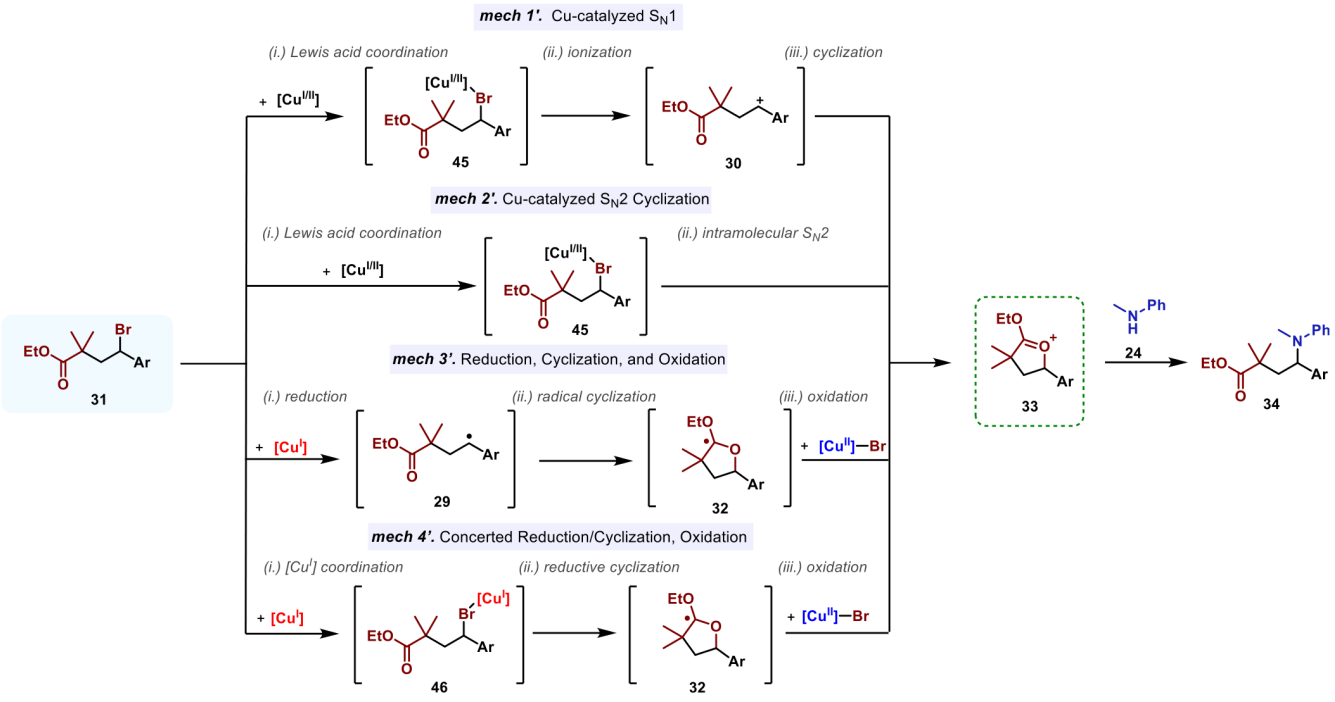

First, we wanted to determine if the reaction is proceeding via **mech 1′** through Hammett and Thorpe-Ingold investigations because if carbocation formation is rate-determining, we would anticipate a large negative ρ value and negligible impact of α-substituents. Plotting the log $[k_{int}(X)/k_{int}(H)]$ vs σ^+, measured in the presence of 3.5 mol % $[Cu^{II}]$ complex **27**, reveals a ρ value of −1.9 (Figure 6a). The measured rate constants for the amination in the presence of the Cu catalyst is a combination of the catalyzed and uncatalyzed pathways.

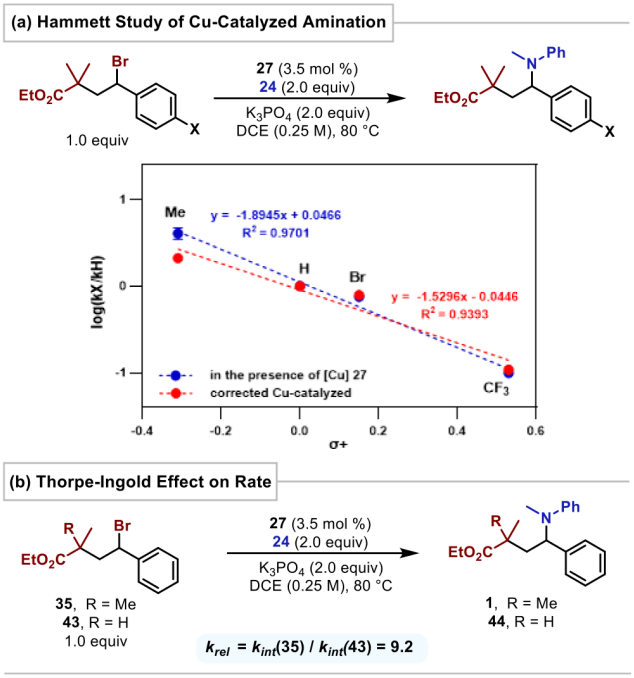

Figure 6. Hammett study and Thorpe-Ingold effect on Cu-catalyzed aminations.

To correct for this, we subtracted the rate constants attributed to the uncatalyzed reaction from those measured in the presence of the copper catalyst. The Hammett plot for the Cu-catalyzed reactions has a ρ value of −1.5 (Figure 6a). This ρ value is similar to that measured in the three-component carboamination reaction (−1.2, Figure 4) and further supports that the ATRA adduct is an intermediate and that the two reactions occur through the same rate-determining steps. Further, we measured the Thorpe-Ingold effect on the Cu-catalyzed amination of **35** and **43**.[41,42] The amination of α,α-dimethyl substrate **35** is 9 times faster than the α-methyl **43** (Figure 6b), consistent with cyclization occurring before or at the rate-determining step. The magnitude of the ρ-value and evidence of a Thorpe-Ingold rate enhancement eliminate **mech 1′**.

Next, we sought to distinguish between **mech 2′**, **3′**, and **4′**. When a chiral benzylic bromide is subjected to the Cu-catalyzed amination, **mech 2′** and **mech 4′** are anticipated to be stereospecific, while **mech 3′** would form **3** as a racemic mixture. We subjected enantiomerically enriched **37*** (92% ee) to the amination conditions. At 15 min, a 9% yield of **3** was observed as a racemic mixture. Further, the remaining starting material was fully epimerized (Scheme 10a). This indicates that racemization of **37*** is rapid in the presence of the Cu-catalyst and suggests that the ATRA adduct and the benzylic radical are in fast equilibrium.[44] To confirm the reversible reduction of **37**, we performed crossover experiments. Subjecting **37** to the carboamination conditions in the presence of 2 equiv *p*-CF_3-styrene (**36**) leads to the formation of **47** and **48**, as observed by LCMS (Scheme 10b).[45] As such, we cannot definitively eliminate any of the remaining mechanistic pathways given this rapid epimerization.

Mech 3′ involves a 5-*endo*-trig cyclization of **29** to afford acetal radical **32** (Scheme 9). The rapid racemization of **37*** (Scheme 10a) is consistent with this mechanism. DFT calculations were employed to investigate this possible

https://doi.org/10.1021/jacs.4c08945
J. Am. Chem. Soc. 2024, 146, 25176−25189

Scheme 10. Investigations Supporting Reversible ATRA Formation

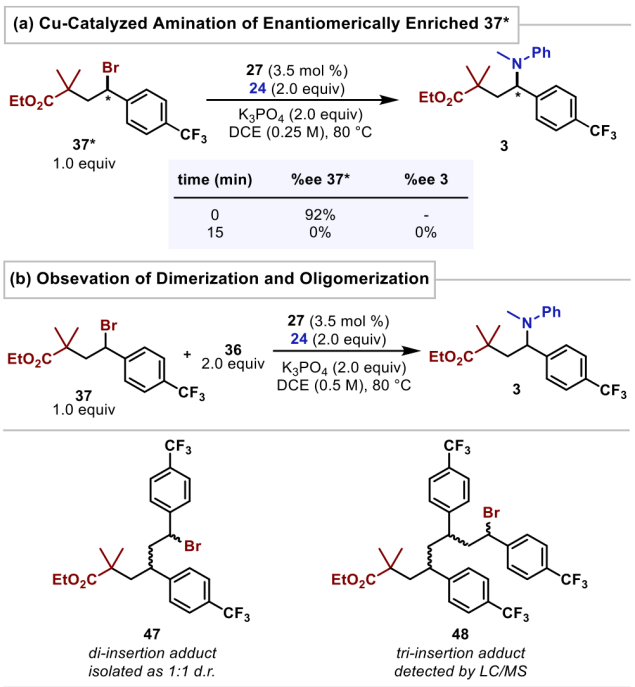

Scheme 11. DFT Calculation for Clamshell Conformation and Radical Cyclization of Benzylic Radical

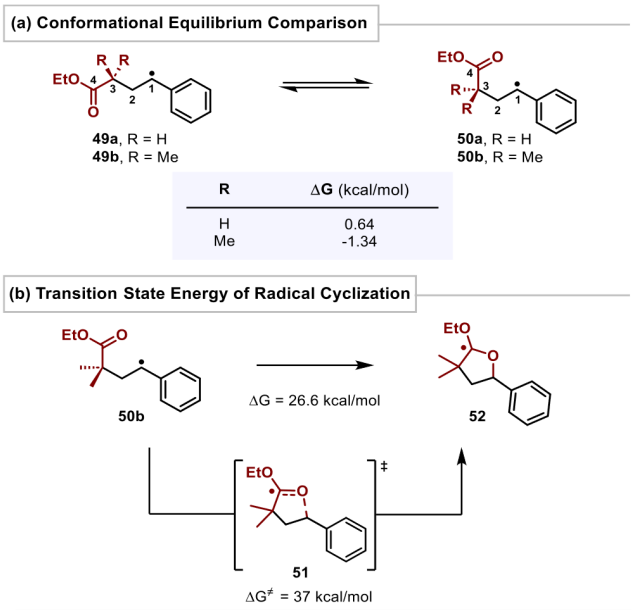

pathway. Interestingly, substitution on the chain (α-carbon) leads to a significant change in the ground state conformation. The unsubstituted chain favors the staggered conformation, thus minimizing gauche interactions. As shown in Scheme 11a, the addition of two methyl groups promotes a conformational change to a "clamshell" conformation such that the carbonyl is gauche to the benzylic radical **50b** ($\Delta G = -1.34$ kcal/mol). As all rotamers around the C2−C3 bond have similar gauche interactions, the lower energy of clamshell conformation **50b** is indicative of a stabilizing interaction between the carbonyl and the benzylic radical. This conformational bias could facilitate the subsequent cyclization. However, the calculated transition state **51** has a $\Delta G^{\ddagger}$ of 37 kcal/mol. This energy barrier is significantly higher than that of the background reaction ($\Delta G^{\ddagger}$ = 20.2 kcal/mol; Scheme 11b) and implies that **mech 3′** is unlikely to occur under the reaction conditions.

Our remaining two mechanisms both involve coordination of the [Cu] catalyst to the benzylic bromide, followed by either S_N2 (**mech 2′**) or reductive cyclization and subsequent oxidation (**mech 4′**). Despite the lower Lewis basicity of the bromide relative to the ester, the coordination of the [Cu^I] to the benzylic bromide is requisite for the reduction of the alkyl halide.[46] DFT analysis was conducted to gain insight into these two possible mechanisms. Despite significant effort, we were unable to calculate a transition state for either of these proposed Cu-catalyzed cyclizations. However, DFT analysis of the intermediates involving [Cu^I] and [Cu^{II}] complexes shows that ΔG (ΔH) of the cyclic acetal radical and [Cu^{II}(dtbbpy)$_2$Br]$^+$ are 23.8 (23.4) kcal/mol higher in energy than ATRA intermediate **35** and [Cu^I(dtbbpy)$_2$]$^+$ (Scheme 12), while the calculated transition state energy ($\Delta G^{\ddagger}$) for the background reaction of **35** to go directly to **33** (X = H) is 20.2 kcal/mol (Scheme 8c). This suggests that the cyclic acetal radical is energetically unfavorable and eliminates **mech 4′**. Moreover, the results also support **mech 2′**, in which the Lewis acid catalyst would serve to lower the $\Delta G^{\ddagger}$ for intramolecular substitution upon coordination to the bromide.

Scheme 12. DFT Analysis for [Cu]-Assisted Radical Cyclization

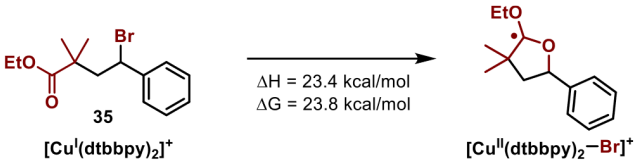

Scheme 13. Zn-Catalyzed Amination of Enantiomerically Enriched ATRA Adduct 37*

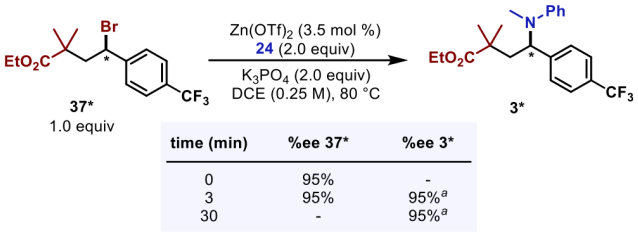

[a]Approximate % ee; see Supporting Information for more details.

To confirm if Lewis acids catalyze the intramolecular S_N2 reaction (**mech 2′**), we employed a nonredox active Lewis acid, Zn(OTf)$_2$ (3.5 mol %), to the uncatalyzed amination conditions. This reaction is significantly faster than the background reaction ($k_{Zn(II)}/k_{background}$ = 337). Further, the reaction is stereospecific, as subjecting enantiomerically enriched **37*** (95% ee) to the Zn-catalyzed amination affords **3** as a single enantiomer (>95% ee) (Scheme 13).

To further support that the Lewis acids catalyze the substitution, we conducted experiments using benzylic bromides **53a** (X = H) and **53b** (X = CF_3). A slight increase in rate (k_{rel} = 1.1), relative to the background substitution between **53a** and **24**, is seen with 3.5 mol % [Cu] **27**; the rate

https://doi.org/10.1021/jacs.4c08945
J. Am. Chem. Soc. 2024, 146, 25176−25189

enhancement is significantly higher with less reactive **53b** (k_{rel} = 15). Notably, an even greater rate increase is observed with the more Lewis acidic $Zn(OTf)_2$. The relative rates in Scheme 14 are consistent with our Hammett study (Figure 6a), where

Scheme 14. Amination of (1-Bromoethyl)benzene Derivatives

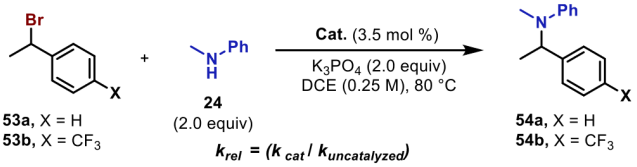

$k_{rel} = (k_{cat} / k_{uncatalyzed})$

Cat.	k_{rel} (53a)	k_{rel} (53b)
none	1.0	1.0
27	1.1	15
$Zn(OTf)_2$	8.7	28

the catalyst has more impact on the rate of the oxocarbenium formation with increasingly electron-deficient ATRA adducts. Combined, these results support that **mech 2′** is operative.

Our mechanistic investigations support that the carboamination reaction is primarily proceeding through **mech 2′**. Notably, as both [Cu^I] and [Cu^{II}] are present in the reaction mixture, as supported by the rapid racemization of enantiomerically enriched **37***, either could serve to catalyze this pathway. To determine if [Cu^I] is an effective Lewis acid catalyst, we investigated its ability to catalyze oxocarbenium formation with an aliphatic alkyl halide **57**. Unactivated, aliphatic alkyl halides have significantly lower reduction potentials than benzylic alkyl halides. For example, 2-bromobutane and (1-bromoethyl)benzene have reduction potentials of −1.21 and −0.46 V vs the saturated calomel electrode, respectively.[47]

Unactivated alkenes undergo iminolactonization reaction with primary amines. With secondary amines, we observed the formation of lactone products. These results indicate that an oxocarbenium intermediate is formed. Like the reaction with styrene, monitoring the iminolactonization of octene over time shows a significant buildup of the ATRA adduct **57**, followed by the formation of the iminolactone **10** (Figure 7a). However, the impact of Lewis acids on the rate is significantly attenuated for these less reactive substrates: the rate of Cu- and Zn-catalyzed iminolactonization is only 10 and 20% faster, respectively, than the uncatalyzed reaction (Figure 7b). As the [Cu^I] complex is unlikely to reduce **57**, there will be a negligible concentration of [Cu^{II}] under these reaction conditions. These results suggest that in our system, [Cu^I] can act as a Lewis acid, assisting S_N2 cyclization of **57**.

Carboamination vs Polymerization. Under our reaction conditions, we typically do not observe significant oligomerization/polymerization despite the formation of ATRA adducts and our catalyst being similar to those used for atom transfer radical polymerization (ATRP).[45,48−50] When 1.0 equiv styrene is used as the alkene coupling partner, no multiple addition adducts are observed by LCMS. This suggests that the carboamination reaction is faster than ATRP. Side products involving multiple radical additions to styrene (**19**) are observed when excess alkene (>10 equiv) is added to the reaction. Electron-deficient alkenes, e.g., *p*-CF_3-styrene (**36**), are prone to undergo oligomerization processes and often afford the carboamination products in lower yields. The radical

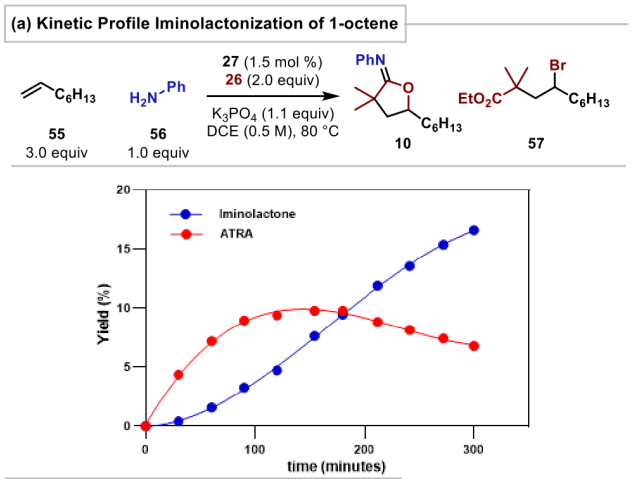

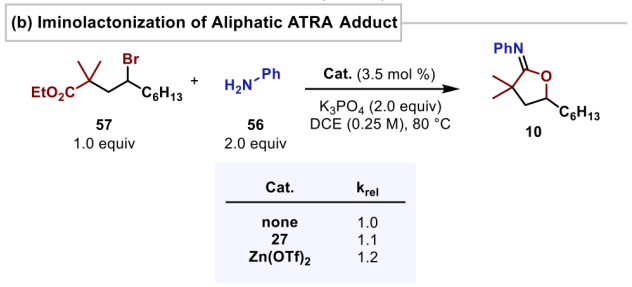

Cat.	k_{rel}
none	1.0
27	1.1
$Zn(OTf)_2$	1.2

Figure 7. Iminolactonization of octene.

Scheme 15. Cu-Catalyzed Three-Component Carboamination of *p*-CF_3-Styrene

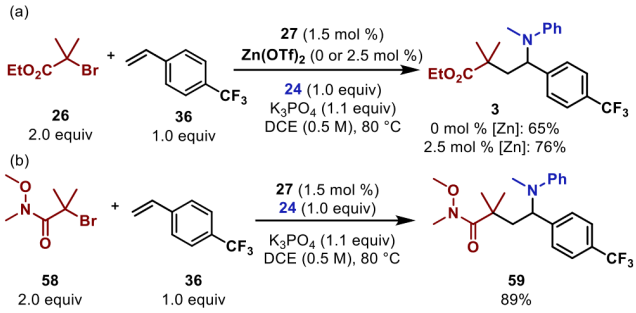

addition to electron-deficient styrene derivatives is known to be fast due to the polarity match between the nucleophilic radical and electrophilic alkenes.[45,48−50] When comparing styrene to *p*-CF_3-styrene, we observe that early in the reaction, the total yield of carboamination products (**1** and **3**) and ATRA intermediates (**35** and **37**) is lower with styrene than with *p*-CF_3-styrene: the combined yields are 8 and 20% at 10 min, respectively (Figure 2a,b). We hypothesized that oligomerization could be minimized by increasing the rate of cyclization by adding a Lewis acidic cocatalyst. Indeed, the addition of 2.5 mol % $Zn(OTf)_2$ to our optimized conditions moderately increases the yield of **3** to 76% (Scheme 15a). Alternatively, the more nucleophilic Weinreb amide **58** significantly improves the reactivity, as **59** is formed in 89% isolated yield (Scheme 15b).

Proposed Catalytic Cycle. Combined, these mechanistic investigations support that the Cu-catalyzed three-component carboamination reaction proceeds through the catalytic cycle shown in Scheme 16. The reaction begins with the reduction

https://doi.org/10.1021/jacs.4c08945
J. Am. Chem. Soc. 2024, 146, 25176−25189

Scheme 16. Proposed Mechanism

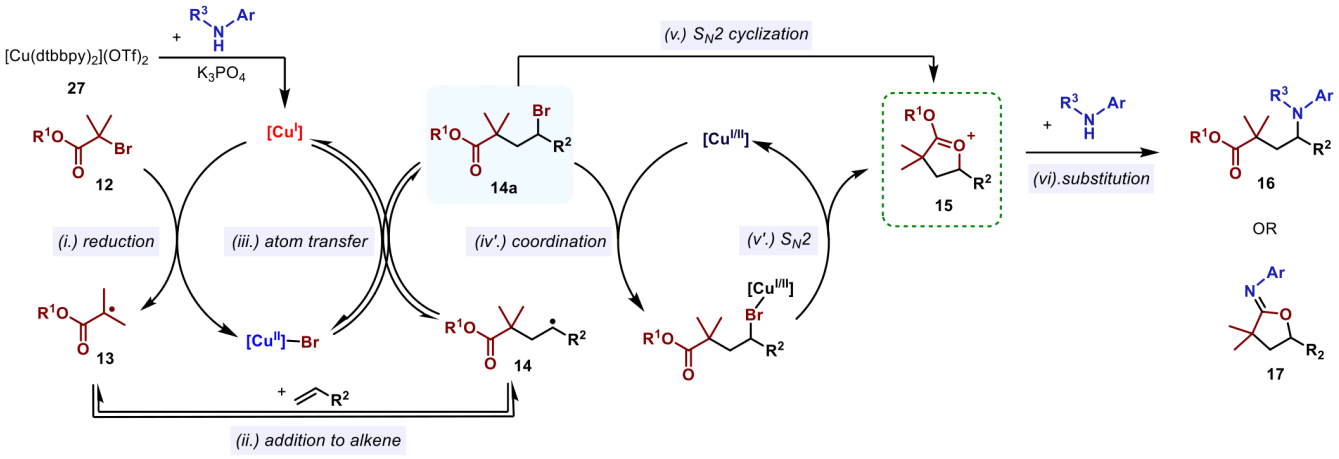

Scheme 17. Degree of Substitution and the Electronic Nature of the Nucleophile's Influence on Product Selectivity

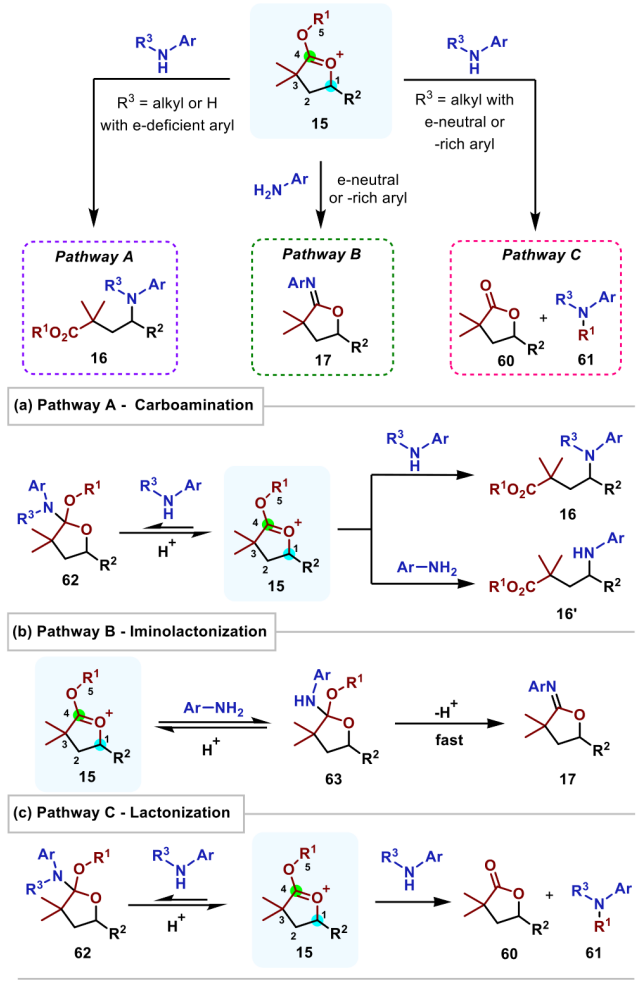

of the [Cu^{II}] precatalyst by aniline and K_3PO_4, generating [Cu^{I}] *in situ*. Then, (i) the α-bromoester is reduced by [Cu^{I}] to generate carbon-centered radical **13** and the [Cu^{II}]–Br complex. Subsequent (ii) addition of the radical **13** to the olefin affords the radical addition adduct **14**, which is (iii) in equilibrium with ATRA intermediate **14a** and [Cu^{I}]. The key oxocarbenium intermediate **15** is generated predominantly by (iv′–v′) Cu-assisted cyclization by the ester onto the benzylic bromide. In the reactions with electron-rich vinyl arenes and unactivated alkenes, (v) uncatalyzed S_N2 cyclization of the ATRA adduct **14a** is dominant. Finally, (vi) the resulting oxocarbenium undergoes nucleophilic attack by an amine to afford the γ-aminoester **16** or γ-iminolactone **17**.

Chiral Auxiliaries. The proposed catalytic cycle explains the styrene-dependent diastereoselectivity observed with Evan's auxiliaries (Scheme 3b). The ATRA intermediate likely forms as a near 1:1 mixture, as the remote stereocenter will have little impact on diastereodetermining C–Br bond formation. As the stereodetermining step is oxocarbenium formation, the relative rates of the racemization of the benzylic bromide, via reduction of the C–Br bond and subsequent atom transfer (k_{act}/k_{deact}), and the intramolecular S_N2 (k^{v} and $k^{v'}$) determine the overall diastereoselectivity. With *p*-MeO groups, the rate of oxocarbenium formation is faster than racemization, resulting in the carboamination product with the lowest diastereoselectivity (1.3:1). Conversely, the *p*-CF_3 substituent increases the rate of racemization, slows the rate of oxocarbenium formation, and therefore improves the diastereoselectivity to 8:1 through a dynamic kinetic transformation.[51]

Reactivity of the Oxocarbenium Intermediate. Next, we focused our efforts on improving our understanding of the oxocarbenium intermediate. It has three electrophilic sites, C1, C4, and C5 (Scheme 17), which afford the carboamination, iminolactone, or lactone product, respectively, via pathways A, B, or C. Both the nucleophile and the alkene impact the relative rates of the pathways and, therefore, the observed product distribution.

Pathway A—Carboamination. The nucleophilic opening at C1 affords the carboamination product. This pathway is preferred with *N*-alkyl anilines as well as electron-deficient primary anilines, such as 2,3,4,5,6-pentafluoroaniline and *p*-nitroaniline. This is consistent with a reversible nucleophilic attack at C4 and an irreversible attack at C1 (Scheme 17a). Secondary amines cannot condense to form the iminolactone; thus, the carboamination product forms selectively. Electron-deficient primary anilines are good leaving groups and thus similarly reversible.

Electron-rich alkenes, e.g., *p*-MeO-styrene and β-methyl-*p*-MeO- styrene, afford the carboamination product over the iminolactone, with a variety of anilines.[4] Interestingly, with *N*-methylaniline, the carboarylation product is also observed. As

https://doi.org/10.1021/jacs.4c08945
J. Am. Chem. Soc. 2024, 146, 25176–25189

electron-donating groups are known to promote S_N2 reactions, we hypothesize that this may be due to the stabilization of the partial positive charge at the benzylic position, increasing the electrophilicity of C1 relative to C4. Alternatively, these electron-rich styrene derivatives may undergo an S_N1 reaction with a dynamic equilibrium between oxocarbenium and the acyclic carbocation intermediate.

As the DFT calculations suggest that the free carbocation is 7.2 kcal/mol less stable than the oxocarbenium intermediate, we sought to determine which pathway occurs. When β-methylstyrene is subjected to the carboamination reaction, we observe the selective formation of *trans*-iminolactone with aniline, suggesting that the *trans*-oxocarbenium intermediate forms selectively.[4] When β-methyl *p*-MeO-styrene **64** is subjected to the carboamination reaction with aniline, we observe the selective formation of the carboamination product **66** as a single diastereomer (>20:1 dr) in 61% isolated yield. Subsequent basic cyclization of the lactam with NaH affords *cis*-lactam **67** (Scheme 18). This is consistent with the

Scheme 18. Templated S_N1 Amination of β-Methyl-*p*-methoxy Styrene

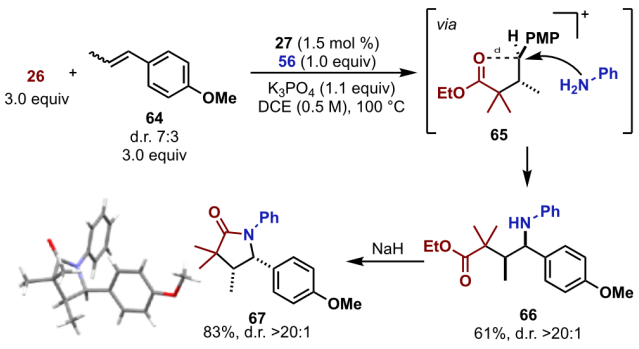

formation of the *trans*-oxocarbenium intermediate followed by a stereoinvertive substitution—pathway A. The increased electrophilicity of C1 vs C4 and the observed EAS products suggest a highly asynchronous transition state.

Pathway B—Iminolactonization. Selective iminolactonization is observed with electron-rich primary amines and anilines, electron-neutral or electron-deficient styrenes, as well as unactivated olefins. This is consistent with a fast nucleophilic attack on C4, followed by the loss of HOR[1] (Scheme 17b). This mechanism is favored with amines that efficiently eliminate an HOR[1] from intermediate **15**.

Pathway C—Lactonization. Nucleophilic attack at C5, a minor pathway in most of our carbofunctionalization reactions, affords the lactone byproduct. It forms when C5 is the most electrophilic site of the oxocarbenium, as observed in Scheme 3. Depending upon the substitution of C5, it can occur either through S_N1, S_N2, E1, or E2. Under our original carboamination reaction conditions, α-olefins undergo selective iminolactonization with primary amines and lactonization with secondary amines. Secondary amine nucleophiles cannot undergo condensation to afford iminolactone. With unactivated alkenes, C1 is tertiary and not benzylic; thus, nucleophilic attack occurs selectively at C5, the primary electrophile (Scheme 19).

Carboamination of α-Olefins. The inability of α-olefins to participate in the carboamination reaction is a significant limitation. We hypothesized that we could promote carboamination over lactonization by reducing the electrophilicity of C5 relative to C1 and that *neo*-pentyl 2-bromo-*iso*butyrate **71** would be a superior coupling partner (Scheme 20a). *neo*-Pentylic carbons are slow to undergo both S_N1 and S_N2 reactions relative to secondary carbons. Indeed, this strategy proved successful, as carboamination products (**75**−**80**) are formed selectively (Scheme 20b). It is important to note that a high temperature (110 °C) is required to promote the reaction. This increase in reaction temperature leads to a concomitant increase in the formation of elimination side-products. Since negligible elimination products are observed with styrene derivatives, we hypothesize that exo C−H bonds, which can align with C−O σ^*, are responsible for this undesired reactivity. Indeed, characterization of the elimination product reveals that the δ,γ-unsaturated esters **74** form selectively.

Scheme 19. Lactonization of Octene

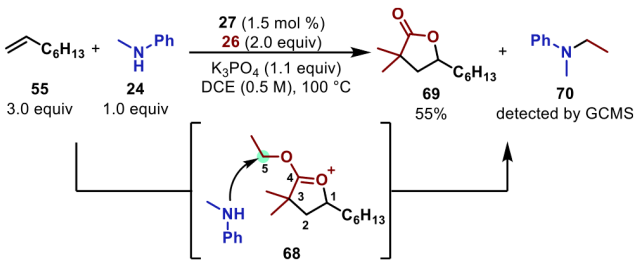

Scheme 20. Carboamination of α-Olefins[a]

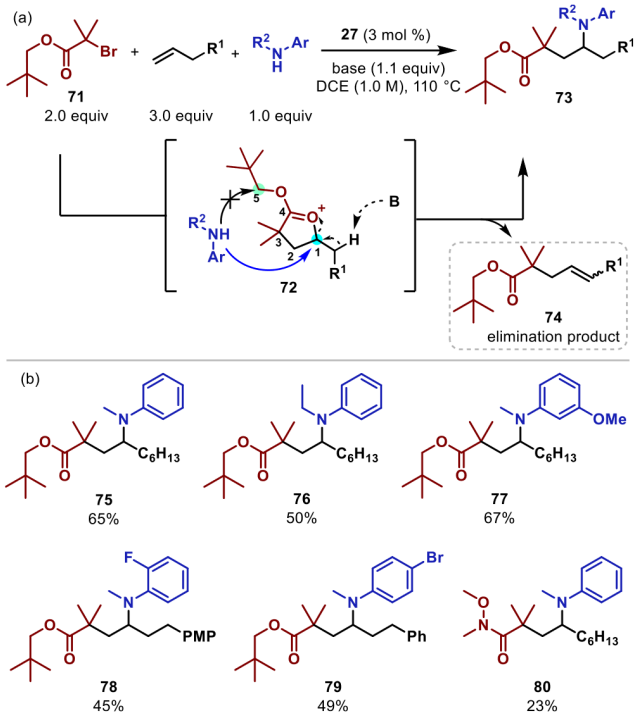

[a]See Supporting Information for reaction conditions.

One-Pot, Two-Step Carbofunctionalization. Our initial carboamination reaction was limited to α-halo carbonyls and secondary or electron-deficient anilines. We hypothesized that a complementary scope for amines and alkyl halides could be achieved via ATRA and subsequent intermolecular substitution. While ATRA reactions are known, current methods are still limited in the diversity of olefin and alkyl halide coupling

https://doi.org/10.1021/jacs.4c08945
J. Am. Chem. Soc. 2024, 146, 25176−25189

partners that participate.[52−57] As ATRA adducts were detected with many alkenes throughout our mechanistic studies, Cu complex **27** may serve as an excellent catalyst for this transformation. To generate the active [Cu^{I}] catalyst, a substoichiometric amount (10 mol %) of *N*-methylaniline and K_3PO_4 is needed. A wide range of readily reducible secondary and tertiary alkyl halide radical precursors participate under the reaction conditions with both vinylarenes and unactivated alkenes to afford the ATRA products **81**−**89** in good to excellent yields (Scheme 21a). Under slightly modified conditions, employing tris(2-pyridylmethyl)amine to generate a more active Cu catalyst,[46] primary alkyl halides couple with both activated and unactivated alkenes (**90**−**92**). Notably, the resulting ATRA products can participate in substitution reactions with a variety of nucleophiles without the necessity of an oxocarbenium intermediate, as demonstrated by the one-pot, two-step protocol developed (Scheme 21b). A variety of nucleophiles, including thiophenol, sodium azide, primary anilines, and primary and secondary alkyl amines, participate in affording carbofunctionalization products **93**−**98**.

Scheme 21. Cu-Catalyzed ATRA of Vinyl Arenes and One-Pot, Two-Step Carbofunctionalization[a]

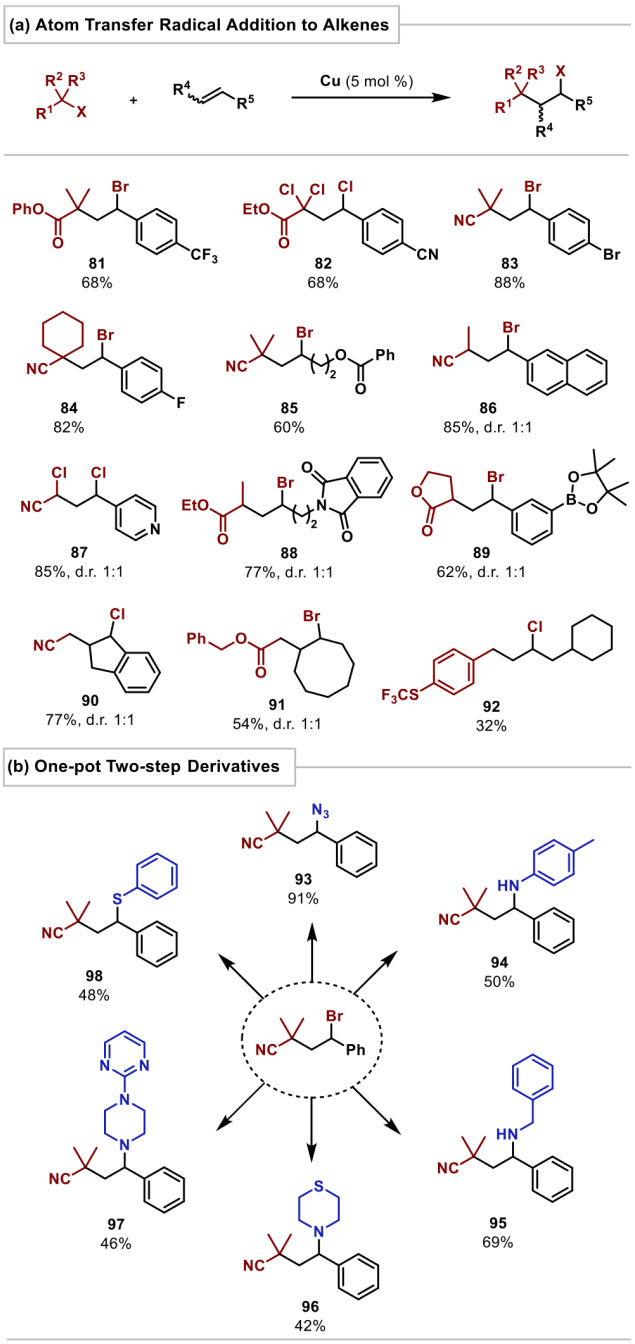

[a]See Supporting Information for reaction conditions.

CONCLUSIONS

The mechanistic investigations described herein give substantial insight into the three-component Cu-catalyzed carboamination of olefins with α-halo carbonyls and secondary anilines. These reactions proceed through a key oxocarbenium intermediate, which is formed via ATRA and subsequent S_N2. The resulting oxocarbenium undergoes nucleophilic attack by the amine to afford the γ-aminoester **16** or γ-iminolactone **17**. With our improved understanding of the catalytic cycle, we were able to develop conditions that allow for the selective carboamination of unactivated alkenes. Further, we successfully developed a general method for Cu-catalyzed ATRA for both vinylarenes and unactivated alkenes with a diversity of reducible alkyl halides, including α-carbonyl, nitrile, and benzylic halides. Our future efforts will focus on the development of stereoselective ATRA and carbofunctionalization reactions. Our mechanistic insights suggest a viable mechanism for asymmetric carboamination via the development of an asymmetric Cu-catalyzed ATRA reaction. Moreover, this work further demonstrates that Cu is an excellent catalyst for ATRA reactions with electronically diverse activated and unactivated alkenes.

ASSOCIATED CONTENT

Supporting Information

The Supporting Information is available free of charge at https://pubs.acs.org/doi/10.1021/jacs.4c08945.

Atomic Coordinates for Geometrically Optimized Complexes (PDF)

Combined NMR Mechanistic Study (ZIP)

Experimental procedures, spectra, mechanistic studies, and summarized optimization (PDF)

Accession Codes

CCDC 2071439 and 2260132 contain the supplementary crystallographic data for this paper. These data can be obtained free of charge via www.ccdc.cam.ac.uk/data_request/cif, or by emailing data_request@ccdc.cam.ac.uk, or by contacting The Cambridge Crystallographic Data Centre, 12 Union Road, Cambridge CB2 1EZ, UK; fax: +44 1223 336033.

AUTHOR INFORMATION

Corresponding Authors

Kami L. Hull − *Department of Chemistry, University of Texas at Austin, Austin, Texas 78712, United States;* orcid.org/0000-0003-3102-2686; Email: kamihull@austin.utexas.edu

Katie R. Mitchell-Koch − *Department of Chemistry and Biochemistry, Wichita State University, Wichita, Kansas 67260-0051, United States;* orcid.org/0000-0002-9173-3677; Email: katie.mitchellkoch@umanitoba.ca

https://doi.org/10.1021/jacs.4c08945
J. Am. Chem. Soc. 2024, 146, 25176−25189

Authors

Tam D. Ho − *Department of Chemistry, University of Texas at Austin, Austin, Texas 78712, United States*

Byung Joo Lee − *Department of Chemistry, University of Texas at Austin, Austin, Texas 78712, United States*

Travis L. Buchanan − *Department of Chemistry, University of Texas at Austin, Austin, Texas 78712, United States*

Micah E. Heikes − *Department of Chemistry and Biochemistry, Wichita State University, Wichita, Kansas 67260-0051, United States*

Ryan M. Steinert − *Department of Chemistry and Biochemistry, Wichita State University, Wichita, Kansas 67260-0051, United States;* orcid.org/0000-0002-2157-6362

E. Grace Milem − *Department of Chemistry, University of Texas at Austin, Austin, Texas 78712, United States;* orcid.org/0009-0001-7467-1160

Sean T. Goralski − *Department of Chemistry, University of Texas at Austin, Austin, Texas 78712, United States;* orcid.org/0000-0002-4169-338X

Ya-Nong Wang − *Department of Chemistry, University of Texas at Austin, Austin, Texas 78712, United States;* orcid.org/0000-0002-5838-3855

SangHyun Lee − *Department of Chemistry, University of Texas at Austin, Austin, Texas 78712, United States;* orcid.org/0000-0001-9519-137X

Vincent M. Lynch − *Department of Chemistry, University of Texas at Austin, Austin, Texas 78712, United States*

Michael J. Rose − *Department of Chemistry, University of Texas at Austin, Austin, Texas 78712, United States;* orcid.org/0000-0002-6960-6639

Complete contact information is available at: https://pubs.acs.org/10.1021/jacs.4c08945

Author Contributions

[§]T.D.H. and B.J.L. have contributed equally. All authors have given approval to the final version of the manuscript.

Funding

KLH thanks the NIH (R35 GM125029), the Sloan Foundation (FG-2016−6568), the Welch Foundation (F-1994−20220331), Amgen, Novartis, Eli Lilly, and the University of Texas at Austin for their generous support. KRMK thanks the NSF (1738708) for their generous support. MJR acknowledges the Welch Foundation (F-1822).

Notes

The authors declare no competing financial interest.

■ ACKNOWLEDGMENTS

We would like to thank the University of Texas at Austin's NMR, X-ray crystallography, and mass spectrometry core facilities and Joseph Willoughby for assistance with the X-ray structure image file and Jeremy Brinker for his assistance with cyclic voltammetry.

■ REFERENCES

(1) Wolfe, J. P. Synthesis of Saturated Heterocycles via Metal-Catalyzed Alkene Carboamination or Carboalkoxylation Reactions. In *Synthesis of Heterocycles via Metal-Catalyzed Reactions that Generate One or More Carbon-Heteroatom Bonds*; Wolfe, J. P., Ed.; Springer: Berlin Heidelberg, 2013; pp 1−37.*Topics in Heterocyclic Chemistry*

(2) Chemler, S. R.; Fuller, P. H. Heterocycle synthesis by copper facilitated addition of heteroatoms to alkenes, alkynes and arenes. *Chem. Soc. Rev.* **2007**, *36* (7), 1153−1160.

(3) Jiang, H.; Studer, A. Intermolecular radical carboamination of alkenes. *Chem. Soc. Rev.* **2020**, *49* (6), 1790−1811.

(4) Gockel, S. N.; Buchanan, T. L.; Hull, K. L. Cu-Catalyzed Three-Component Carboamination of Alkenes. *J. Am. Chem. Soc.* **2018**, *140* (1), 58−61.

(5) Lira, R.; Wolfe, J. P. Palladium-catalyzed synthesis of N-aryl-2-benzylindolines via tandem arylation of 2-allylaniline: control of selectivity through in situ catalyst modification. *J. Am. Chem. Soc.* **2004**, *126* (43), 13906−13907.

(6) Ney, J. E.; Wolfe, J. P. Palladium-catalyzed synthesis of N-aryl pyrrolidines from gamma-(N-Arylamino) alkenes: evidence for chemoselective alkene insertion into Pd−N bonds. *Angew. Chem., Int. Ed. Engl.* **2004**, *43* (27), 3605−3608.

(7) Bertrand, M. B.; Wolfe, J. P. Stereoselective synthesis of N-protected pyrrolidines via Pd-catalyzed reactions of γ-(N-acylamino) alkenes and γ-(N-Boc-amino) alkenes with aryl bromides. *Tetrahedron* **2005**, *61* (26), 6447−6459.

(8) Yang, Q.; Ney, J. E.; Wolfe, J. P. Palladium-catalyzed tandem N-arylation/carboamination reactions for the stereoselective synthesis of N-aryl-2-benzyl pyrrolidines. *Org. Lett.* **2005**, *7* (13), 2575−2578.

(9) Ney, J. E.; Hay, M. B.; Yang, Q.; Wolfe, J. P. Synthesis of N-Aryl-2-allyl Pyrrolidines via Palladium-catalyzed Carboamination Reactions of gamma-(N-Arylamino)alkenes with Vinyl Bromides. *Adv. Synth. Catal.* **2005**, *347* (11−13), 1614−1620.

(10) Garlets, Z. J.; White, D. R.; Wolfe, J. P. Recent Developments in Pd(0)-Catalyzed Alkene Carboheterofunctionalization Reactions. *Asian J. Org. Chem.* **2017**, *6* (6), 636−653.

(11) Sherman, E. S.; Chemler, S. R.; Tan, T. B.; Gerlits, O. Copper(II) acetate promoted oxidative cyclization of arylsulfonyl-o-allylanilines. *Org. Lett.* **2004**, *6* (10), 1573−1575.

(12) Fuller, P. H.; Chemler, S. R. Copper(II) carboxylate-promoted intramolecular carboamination of alkenes for the synthesis of polycyclic lactams. *Org. Lett.* **2007**, *9* (26), 5477−5480.

(13) Zabawa, T. P.; Chemler, S. R. Copper(II) carboxylate promoted intramolecular diamination of terminal alkenes: improved reaction conditions and expanded substrate scope. *Org. Lett.* **2007**, *9* (10), 2035−2038.

(14) Zeng, W.; Chemler, S. R. Copper(II)-catalyzed enantioselective intramolecular carboamination of alkenes. *J. Am. Chem. Soc.* **2007**, *129* (43), 12948−12949.

(15) Sherman, E. S.; Fuller, P. H.; Kasi, D.; Chemler, S. R. Pyrrolidine and piperidine formation via copper(II) carboxylate-promoted intramolecular carboamination of unactivated olefins: diastereoselectivity and mechanism. *J. Org. Chem.* **2007**, *72* (10), 3896−3905.

(16) Piou, T.; Rovis, T. Rhodium-catalysed syn-carboamination of alkenes via a transient directing group. *Nature* **2015**, *527* (7576), 86−90.

(17) Ouyang, X. H.; Li, Y.; Song, R. J.; Li, J. H. Alkylamination of Styrenes with Alkyl N-Hydroxyphthalimide Esters and Amines by $B(C_6H_5)_3$-Facilitated Photoredox Catalysis. *Org. Lett.* **2018**, *20* (21), 6659−6662.

(18) Xiong, Y.; Ma, X.; Zhang, G. Copper-Catalyzed Intermolecular Carboamination of Alkenes Induced by Visible Light. *Org. Lett.* **2019**, *21* (6), 1699−1703.

(19) Lee, S.; Rovis, T. Rh(III)-Catalyzed Three-Component Syn-Carboamination of Alkenes Using Arylboronic Acids and Dioxazolones. *ACS Catal.* **2021**, *11* (14), 8585−8590.

(20) Jiang, H.; Seidler, G.; Studer, A. Carboamination of Unactivated Alkenes through Three-Component Radical Conjugate Addition. *Angew. Chem., Int. Ed. Engl.* **2019**, *58* (46), 16528−16532.

(21) Kennedy-Ellis, J. J.; Boldt, E. D.; Chemler, S. R. Synthesis of Benzylureas and Related Amine Derivatives via Copper-Catalyzed Three-Component Carboamination of Styrenes. *Org. Lett.* **2020**, *22* (21), 8365−8369.

(22) Liu, Z.; Wang, Y.; Wang, Z.; Zeng, T.; Liu, P.; Engle, K. M. Catalytic Intermolecular Carboamination of Unactivated Alkenes via Directed Aminopalladation. *J. Am. Chem. Soc.* **2017**, *139* (32), 11261−11270.

(23) Yasu, Y.; Koike, T.; Akita, M. Intermolecular Amino-trifluoromethylation of Alkenes by Visible-Light-Driven Photoredox Catalysis. *Org. Lett.* **2013**, *15* (9), 2136−2139.
(24) Liu, Y. Y.; Yang, X. H.; Song, R. J.; Luo, S.; Li, J. H. Oxidative 1,2-carboamination of alkenes with alkyl nitriles and amines toward gamma-amino alkyl nitriles. *Nat. Commun.* **2017**, *8*, 14720.
(25) Qian, B.; Chen, S.; Wang, T.; Zhang, X.; Bao, H. Iron-Catalyzed Carboamination of Olefins: Synthesis of Amines and Disubstituted β-Amino Acids. *J. Am. Chem. Soc.* **2017**, *139* (37), 13076−13082.
(26) Gockel, S. N.; Lee, S.; Gay, B. L.; Hull, K. L. Oxidative Three-Component Carboamination of Vinylarenes with Alkylboronic Acids. *ACS Catal.* **2021**, *11* (9), 5166−5171.
(27) Nicely, A. M.; Popov, A. G.; Wendlandt, H. C.; Trammel, G. L.; Kohler, D. G.; Hull, K. L. Cu-Catalyzed Three-Component Carboamination of Electron Deficient Olefins. *Org. Lett.* **2023**, *25* (28), 5302−5307.
(28) Eckenhoff, W. T.; Pintauer, T. Atom transfer radical addition (ATRA) catalyzed by copper complexes with tris[2-(dimethylamino)-ethyl]amine (Me6TREN) ligand in the presence of free-radical diazo initiator AIBN. *Dalton Trans.* **2011**, *40* (18), 4909−4917.
(29) Lin, C. Y.; Coote, M. L.; Gennaro, A.; Matyjaszewski, K. Ab initio evaluation of the thermodynamic and electrochemical properties of alkyl halides and radicals and their mechanistic implications for atom transfer radical polymerization. *J. Am. Chem. Soc.* **2008**, *130* (38), 12762−12774.
(30) Fischer, H.; Radom, L. Factors Controlling the Addition of Carbon-Centered Radicals to Alkenes-An Experimental and Theoretical Perspective. *Angew. Chem., Int. Ed. Engl.* **2001**, *40* (8), 1340−1371.
(31) Kochi, J. K.; Bemis, A. Carbonium ions from alkyl radicals by electron transfer. *J. Am. Chem. Soc.* **1968**, *90* (15), 4038−4051.
(32) Jenkins, C. L.; Kochi, J. K. Homolytic and ionic mechanisms in the ligand-transfer oxidation of alkyl radicals by copper(II) halides and pseudohalides. *J. Am. Chem. Soc.* **1972**, *94* (3), 856−865.
(33) Kochi, J. K.; Bemis, A.; Jenkins, C. L. Mechanism of electron transfer oxidation of alkyl radicals by copper(II) complexes. *J. Am. Chem. Soc.* **1968**, *90* (17), 4616−4625.
(34) Ho, T. D.; Lee, B. J.; Tan, C.; Utley, J. A.; Ngo, N. Q.; Hull, K. L. Efficient Synthesis of α-Haloboronic Esters via Cu-Catalyzed Atom Transfer Radical Addition. *J. Am. Chem. Soc.* **2023**, *145* (50), 27230−27235.
(35) Golden, D. L.; Zhang, C.; Chen, S.-J.; Vasilopoulos, A.; Guzei, I. A.; Stahl, S. S. Benzylic C−H Esterification with Limiting C−H Substrate Enabled by Photochemical Redox Buffering of the Cu Catalyst. *J. Am. Chem. Soc.* **2023**, *145* (17), 9434−9440.
(36) Hu, H.; Chen, S.-J.; Mandal, M.; Pratik, S. M.; Buss, J. A.; Krska, S. W.; Cramer, C. J.; Stahl, S. S. Copper-catalysed benzylic C−H coupling with alcohols via radical relay enabled by redox buffering. *Nat. Catal.* **2020**, *3* (4), 358−367.
(37) Ribelli, T. G.; Lorandi, F.; Fantin, M.; Matyjaszewski, K. Atom Transfer Radical Polymerization: Billion Times More Active Catalysts and New Initiation Systems. *Macromol. Rapid Commun.* **2019**, *40* (1), No. e1800616.
(38) Eckenhoff, W. T.; Pintauer, T. Copper Catalyzed Atom Transfer Radical Addition (ATRA) and Cyclization (ATRC) Reactions in the Presence of Reducing Agents. *Catal. Rev.* **2010**, *52* (1), 1−59.
(39) Liu, D.; Tang, S.; Yi, H.; Liu, C.; Qi, X.; Lan, Y.; Lei, A. Carbon-Centered Radical Addition to O−C of Amides or Esters as a Route to C−O Bond Formations. *Chem. Eur. J.* **2014**, *20* (47), 15605−15610.
(40) Denegri, B.; Matić, M.; Vaško, M. Mechanism of solvolysis of substituted benzyl chlorides in aqueous ethanol. *Tetrahedron* **2022**, *103*, 132548.
(41) Kaneti, J.; Kirby, A. J.; Koedjikov, A. H.; Pojarlieff, I. G. Thorpe−Ingold effects in cyclizations to five-membered and six-membered rings containing planar segments. The rearrangement of N(1)-alkyl-substituted dihydroorotic acids to hydantoinacetic acids in base. *Org. Biomol. Chem.* **2004**, *2* (7), 1098−1103. 10.1039/B400248B
(42) Beesley, R. M.; Ingold, C. K.; Thorpe, J. F. CXIXCXIX—The formation and stability of spiro-compounds. Part I. spiro-Compounds from cyclohexane. *J. Chem. Soc., Trans.* **1915**, *107* (0), 1080−1106. 10.1039/CT9150701080
(43) Evans, D. A.; Rovis, T.; Johnson, J. S. Chiral copper (II) complexes as Lewis acids for catalyzed cycloaddition, carbonyl addition, and conjugate addition reactions. *Pure Appl. Chem.* **1999**, *71* (8), 1407−1415.
(44) Matyjaszewski, K. Atom Transfer Radical Polymerization (ATRP): Current Status and Future Perspectives. *Macromolecules* **2012**, *45* (10), 4015−4039.
(45) Qiu, J.; Matyjaszewski, K. Polymerization of Substituted Styrenes by Atom Transfer Radical Polymerization. *Macromolecules* **1997**, *30* (19), 5643−5648.
(46) Fang, C.; Fantin, M.; Pan, X.; de Fiebre, K.; Coote, M. L.; Matyjaszewski, K.; Liu, P. Mechanistically Guided Predictive Models for Ligand and Initiator Effects in Copper-Catalyzed Atom Transfer Radical Polymerization (Cu-ATRP). *J. Am. Chem. Soc.* **2019**, *141* (18), 7486−7497.
(47) Isse, A. A.; Gennaro, A.; Lin, C. Y.; Hodgson, J. L.; Coote, M. L.; Guliashvili, T. Mechanism of carbon-halogen bond reductive cleavage in activated alkyl halide initiators relevant to living radical polymerization: theoretical and experimental study. *J. Am. Chem. Soc.* **2011**, *133* (16), 6254−6264.
(48) Subramanian, H.; Landais, Y.; Sibi, M. P. *4.12 Radical Addition Reactions*. Second ed.; Elsevier Ltd, 2014; pp 699−741.
(49) Giese, B. Formation of C−C Bonds by Addition of Free Radicals to Alkenes. *Angew. Chem. Int. Edit* **1983**, *22* (10), 753−764.
(50) Parsaee, F.; Senarathna, M. C.; Kannangara, P. B.; Alexander, S. N.; Arche, P. D. E.; Welin, E. R. Radical philicity and its role in selective organic transformations. *Nat. Rev. Chem* **2021**, *5* (7), 486−499.
(51) Huerta, F. F.; Minidis, A. B. E.; Bäckvall, J.-E. Racemisation in asymmetric synthesis. Dynamic kinetic resolution and related processes in enzyme and metal catalysis. *Chem. Soc. Rev.* **2001**, *30* (6), 321−331. 10.1039/B105464N
(52) Chen, F.; Xu, X.-H.; Qing, F.-L. Photoredox-Catalyzed Addition of Dibromofluoromethane to Alkenes: Direct Synthesis of 1-Bromo-1-fluoroalkanes. *Org. Lett.* **2021**, *23* (6), 2364−2369.
(53) Granados, A.; Dhungana, R. K.; Sharique, M.; Majhi, J.; Molander, G. A. From Styrenes to Fluorinated Benzyl Bromides: A Photoinduced Difunctionalization via Atom Transfer Radical Addition. *Org. Lett.* **2022**, *24* (26), 4750−4755.
(54) Nguyen, J. D.; Tucker, J. W.; Konieczynska, M. D.; Stephenson, C. R. J. Intermolecular Atom Transfer Radical Addition to Olefins Mediated by Oxidative Quenching of Photoredox Catalysts. *J. Am. Chem. Soc.* **2011**, *133* (12), 4160−4163.
(55) Tappin, N. D. C.; Renaud, P. Methyl Radical Initiated Kharasch and Related Reactions. *Adv. Syn. Catal.* **2021**, *363* (1), 275−282.
(56) Wallentin, C. J.; Nguyen, J. D.; Finkbeiner, P.; Stephenson, C. R. Visible light-mediated atom transfer radical addition via oxidative and reductive quenching of photocatalysts. *J. Am. Chem. Soc.* **2012**, *134* (21), 8875−8884.
(57) Kostromitin, V. S.; Zemtsov, A. A.; Kokorekin, V. A.; Levin, V. V.; Dilman, A. D. Atom-transfer radical addition of fluoroalkyl bromides to alkenes via a photoredox/copper catalytic system. *Chem. Commun.* **2021**, *57* (42), 5219−5222.

https://doi.org/10.1021/jacs.4c08945
J. Am. Chem. Soc. 2024, 146, 25176−25189